Investigations of the Oxidative Disassembly of Fe−S Clusters in *Clostridium pasteurianum* 8Fe Ferredoxin Using Pulsed-Protein-Film Voltammetry†

Raúl Camba and Fraser A. Armstrong*

Inorganic Chemistry Laboratory, Oxford University, South Parks Road, Oxford OX1 3QR, England

Received April 12, 2000; Revised Manuscript Received May 25, 2000

ABSTRACT: Rapid responses of biological [4Fe-4S] clusters to conditions of oxidative stress have been studied by protein-film voltammetry by using precise pulses of electrode potential to trigger reactions. Investigations with *Clostridium pasteurianum* 8Fe ferredoxin exploit the fact that [3Fe-4S] clusters display a characteristic pattern of voltammetric signals, so that their appearance and disappearance after an oxidative pulse can be tracked unambiguously under electrochemical control. Adsorbed to monolayer coverage at a graphite electrode, the protein initially shows a strong signal (B′) at −0.36 V vs standard hydrogen electrode due to two $[4Fe\text{-}4S]^{2+/+}$ clusters at similar potentials. Short square pulses (0.1−5 s) to potentials in the range 0.5−0.9 V cause extensive loss of B′, and new signals appear (A′and C′) that arise from [3Fe-4S] species (+/0 and 0/2- couples). The A′ and B′ intensities quantify transformations which are induced by the pulse and which occur subsequently when more reducing conditions are restored. Optimal [3Fe-4S] formation (in excess over [4Fe-4S]) is achieved with a 3-s pulse to 0.7 V, following which there is rapid partial recovery to yield a 1:1 3Fe:4Fe ratio, consistent with 7Fe protein. Thus, a 6Fe protein is formed, but one of the clusters is rapidly repaired. The [3Fe-4S]:[4Fe-4S] ratio follows a bell-shaped curve spanning the same potential range that defines complete loss of signals, while double-pulse experiments show that $[3Fe\text{-}4S]^{+}$ resists further oxidative damage. Oxidative disassembly involves successive one-electron oxidations of [4Fe-4S] (i.e., 2+ → 3+ → 4+), with $[3Fe\text{-}4S]^{+}$ being a relatively stable byproduct, that is, not an intermediate. Disassembly of [3Fe-4S] in the 7Fe protein continues after reducing conditions are restored, with lifetimes depending on oxidation level; thus 1+ (most stable) > 0 > 2−. In the presence of Fe^{2+}, the 0 level is stabilized by conversion back to $[4Fe\text{-}4S]^{2+/+}$. By pulsing in the presence of Zn^{2+}, the [3Fe-4S] clusters that are formed are trapped rapidly as their Zn adducts.

Among the remarkably wide variety of reactions and biological functions of Fe−S clusters (*1*−*18*), particular biological interest now surrounds their roles as sensors (e.g., of Fe levels or reactive oxygen species) in gene expression and enzyme regulation (*9*−*18*). These roles exploit their natural instability and lability. Most obviously, the greater affinity of high-spin Fe(III) for O donors (*19*) means that Fe−S clusters are unstable in contact with water under aerobic/oxidizing conditions. Clusters are obvious primary targets for oxidative stress, and many examples of their partial or complete oxidative disassembly in proteins are now known, both with and without clear biological roles (*9*−*18*).

For simple electron-transfer reactions, [4Fe-4S] clusters generally operate reversibly between 1+ and 2+ levels (although in HiPIPs[1] the 2+ and 3+ oxidation levels are used) (*20*), while further oxidation induces their disassembly. Oxidative degradation of [4Fe-4S] clusters, as understood to date, is summarized in Scheme 1. Partial disassembly to the [3Fe-4S] cuboidal state requires only minor reorganization of the protein ligands and should be readily reversible, whereas transformation to a [2Fe-2S] cluster makes greater conformational demands (*21*).

Scheme 1: Outline of the Oxidative Disassembly of [4Fe-4S] Clusters to Apo States[a]

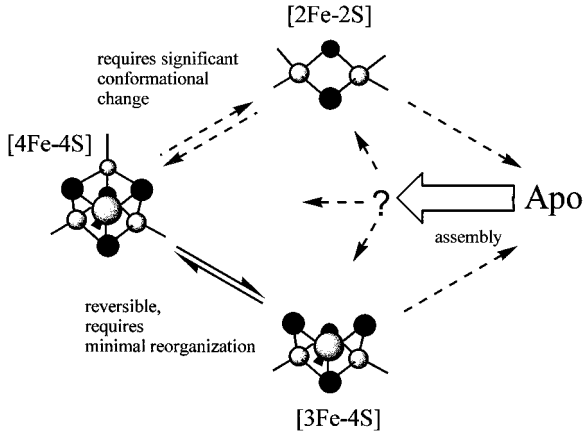

[a] Partial disassembly can occur to [3Fe-4S] or [2Fe-2S] forms.

† This research was supported by the UK EPSRC (Grant GR/J84809) and BBSRC (43/B11675).

* To whom correspondence should be addressed. Phone: 44-1865-272647. Fax: 44-1865-272690. E-mail: fraser.armstrong@icl.ox.ac.uk.

[1] Abbreviations: A, amperes; *Cp*, *Clostridium pasteurinaum*; Fd, ferredoxin; FPLC, fast protein liquid chromatography; HEPES, *N*-[2-hydroxyethyl]piperazine-*N*′-[2-ethanesulfonic acid]; HiPIP, high-potential iron protein; MES, 2-[*N*-morpholino]ethanesulfonic acid; SCE, saturated calomel electrode; SHE, standard hydrogen electrode; TAPS, *N*-tris[hydroxymethyl]methyl-3-aminopropanesulfonic acid; V, volts.

10.1021/bi000832+ CCC: $19.00
Published on Web 08/01/2000

The specific agents of cellular oxidative stress include simple oxygen species such as O_2^- and H_2O_2 (*12*−*15*), but the ways in which they induce cluster damage are uncertain and undoubtedly varied. However, a common and natural basis for discussion is redox energetics, because whatever the nature of the mechanism (*22*), the fact remains that these species can exploit potent oxidizing powers falling in the range of 0.89 V (O_2^-/H_2O_2, one electron) and 1.35 V (H_2O_2/H_2O, two electrons) at pH 7 (*23*).

Examples in which biology is known to exploit this chemistry continue to grow. Those concerning gene expression include the transcription factor FNR (fumarate and nitrate reduction), which controls a network of genes in *E. coli* that express alternative respiratory chains (*17*),[2] and the iron-regulatory protein (IRP), which regulates synthesis of ferritin or transferrin receptor in response to Fe levels (*10, 11, 16*). Binding of FNR to DNA is controlled by conformational changes driven by redox-linked interconversions of [4Fe-4S] and [2Fe-2S] states (*17*), whereas for IRP, binding to iron-responsive elements on messenger RNA depends on prior disassembly of a cluster, [4Fe-4S] or [3Fe-4S], to produce the active apoprotein (*10, 11, 16*). Examples where cluster status may control catalytic activity include mitochondrial aconitase, dihydroxy-acid dehydratases, bacterial fumarases A and B, and also enzymes such as phosphoribosyl-pyrophosphateamidotransferase and endonuclease III, in which an Fe−S cluster is present but is not itself a catalytic site (*3, 10, 12*−*15*). Aconitase is the best-studied example. It is active, provided its [4Fe-4S] cluster is intact, but it is inactivated by degradation to a [3Fe-4S] form because the labile Fe is the site of substrate binding (*10*). This interconversion is reversible and could be used in vivo to control the tricarboxylic acid cycle in response to Fe levels and oxidizing conditions (*12*). Apart from regulation, the oxidative disassembly of Fe−S clusters has wider roles in the Fe cycle and in toxicity, because release of Fe in the presence of oxygen species creates further complications due to Fenton reactions, and total-cluster disassembly may lead to catastrophic effects (*24*). Often perceived as artifactual in many proteins, the [3Fe-4S] cluster might actually play a beneficial role by providing a "safe haven" during oxidative stress, that is, as an all-Fe(III) cuboidal template which limits the extent of Fe release but preserves the form and S content of the biologically active [4Fe-4S] cubane. Thus, so long as Fe is available, the cubane is easily rebuilt once the stress recedes. It is also possible that the initial oxidation event is merely a trigger, producing labile cluster species that break down after reducing conditions are restored.

Important observations have been made with smaller Fe−S proteins (ferredoxins with molecular masses typically of 6−14 kDa) in which [4Fe-4S] clusters are known to degrade to [3Fe-4S] in the presence of O_2 or laboratory oxidants such as ferricyanide [$Fe(CN)_6^{3-}$] (*25*−*32*). Often this process is easily reversed, and reductive treatment of [3Fe-4S] with Fe or other metal ions M, respectively, regenerates [4Fe-4S] or affords routes to heterometal cubanes [M3Fe-4S], the biological occurrence and relevance of which have yet to be established. Treatment of *Clostridium pasteurianum (Cp* Fd*)* 8Fe ferredoxin with $Fe(CN)_6^{3-}$ yields products which have been shown by EPR, MCD, and resonance Raman spectroscopies (*25*) to contain [3Fe-4S] clusters. Later, Bertini and co-workers established by NMR that an isolable product of this reaction is a 7Fe form in which one cluster, termed cluster I, is selectively degraded to [3Fe-4S] (*26*). Thus, although both clusters have similar reduction potentials ($\Delta E = 15$ mV) (*33*), they have differing susceptibilities to oxidative damage. A likely intermediate in disassembly pathways is the superoxidized state $[4Fe\text{-}4S]^{3+}$, which is labile when exposed to solvent. Cowan and co-workers have studied the HiPIP from *Chromatium vinosum*, in which the $[4Fe\text{-}4S]^{3+/2+}$ cluster is shielded from solvent by a tyrosine (Y19) (*34, 35*). Mutations of Y19 (or nearby F66) to small or polar residues increase solvent accessibility, and while there are no major changes in electronic properties or reduction potentials, the normally inert oxidized $[4Fe\text{-}4S]^{3+}$ state is labilized. Degradation proceeds to apoprotein, although a $[3Fe\text{-}4S]^{+}$ species is detected by EPR (*35*).

Given the biological importance of these processes, it is surprising that there is so little quantitative information on the thermodynamics and the kinetics of oxidation-induced cluster disassembly, and there are few guides as to whether any general mechanistic principles apply. The chemistry is seemingly complex and intractible. Obvious problems are how to probe fast reactions and to detect the transient species generated by strong oxidants, or how to measure the reduction potentials defining these transformations. At the very least, it is important to gauge the thermodynamic pressures that are required to trigger or drive breakdown. To help achieve this goal, much can be learned from direct electrochemical methods which have already provided some fresh perspectives on Fe−S chemistry. As past examples, Armstrong and co-workers quantified reversible reactions of the type [M3Fe-4S]/[3Fe-4S] in small ferredoxins (*30, 31, 36*), while Tong and Feinberg used square-wave voltammetry to study interconversion between [3Fe-4S] (inactive) and [4Fe-4S] (active) forms of aconitase (*37*). In these cases, however, the labile Fe is bound not by cysteine but by an atypical O donor such as H_2O (OH^-) or carboxylate, and this replacement undoubtedly influences reactivity (*32*). Here we report about studies to resolve and quantify temporal and energetic dependences of disassembly of the two [4Fe-4S] clusters in *C. pasteurianum* 8Fe ferredoxin, both of which have the all-cysteine ligation more typical of [4Fe-4S] clusters, in either case provided by the classical binding motif -C-x-x-C-x-x-C...CP-.(*4*) Although oxidation processes of 8Fe *Cp* Fd were observed earlier by electrochemical methods using protein solutions (*38*), no details of products or intermediates could be obtained.

We have now extended a method called protein-film voltammetry (PFV) to probe these reactions in a novel way. In PFV (*30, 31, 36, 39*), the protein sample is confined to the electrode, up to monolayer coverage, and active sites yield compact voltammetric signals that are uncomplicated by diffusion. Thus, PFV affords delicate manipulations and precise control and resolution of redox processes and enables detection and quantitation of reactions that are coupled to or control electron transfer. The important new aspect is the

[2] Another transcription factor, SoxR, contains a [2Fe-2S] cluster and controls the cellular response to oxidative stress in *E. coli*. High intracellular superoxide levels activate SoxR, leading to transcription of the target gene *SoxS*. The *SoxS* gene product activates at least 12 genes, whose products metabolize excess superoxide, repair damaged DNA, and restore Krebs-cycle activity. Oxidative stress appears only to oxidize the [2Fe-2S] cluster to the active 2+ level.

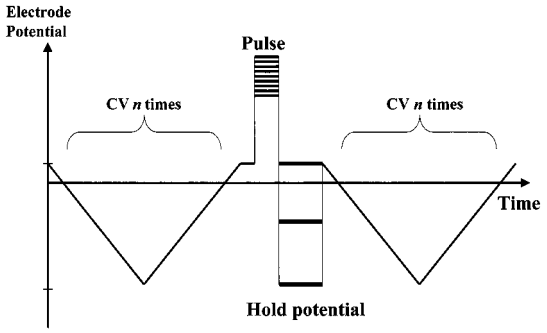

FIGURE 1: Sequence of stages in a pulsed-protein-film voltammetry experiment. Cyclic voltammetry is carried out before and after applying an oxidative pulse of precise potential and duration. Further pulses can be incorporated.

way that the film configuration enables particularly clean triggering of redox-induced reactions. This is because the entire sample can be rapidly perturbed by digital application of oxidative pulses, each of precise potential and duration. The concept is illustrated in Figure 1. After initial cycles to establish a stable electroactive protein film, a square potential pulse is applied, following which cyclic voltammetry, often with fast scan rates, is used to observe the products and monitor their fate. Then, if desired, selective electrode potentials can be applied for fixed periods in order to control further reactions potentiostatically, and reagents can be present in solution to react with products or intermediates (*39*). Numerous options are possible. For example, a second pulse can be applied to activate and probe products resulting from the first.

For Fe−S clusters, the sharp and well-defined signals observed in a protein film serve as in situ reporters for species that are usually distinguished only by low-temperature spectroscopy and which may have just transient existence (*30*, *31*, *36*). In this work, we have exploited the fact that [3Fe-4S] clusters typically display a very distinctive voltammetric pattern, that is, two signals due to the +/0 and 0/2− redox couples (the latter being characteristically sharp), which unambiguously reveals and quantifies their presence, even at trace levels (*40*). Furthermore, for *Cp* Fd, the two clusters in the same molecule serve as a reference for each other, helping to differentiate cluster breakdown from losses due to protein desorption. As we now show, the experiments provide a quantitative guide to the energetics, kinetics, and reversibility of oxidatively triggered cluster disassembly.

EXPERIMENTAL PROCEDURES

General. All experiments were carried out under nitrogen (O_2 < 2 ppm) in a glovebox (Vacuum Atmospheres, Hawthorne CA, or Belle Technology, Dorset, England). Deionized water (18 MΩ cm) was used to prepare all solutions. Reagents used in voltammetry were of the highest purity available and, except for NaCl and sodium acetate (BDH), were obtained from Sigma.

Preparation of Protein Samples. The 8Fe ferredoxin from *C. pasteurianum* (CAMR, Porton Down, England) was isolated using the method described by Moulis and Meyer (*41*). It was purified further by FPLC (Pharmacia, Sweden) using a Mono Q column equilibrated with 50 mM Tris (Tris-[hydroxymethyl]aminomethane) at pH 7.5 and eluting using a 0−1 M NaCl gradient. The purity was established from the A_{390}:A_{280} ratio, which was typically >0.82. A minor fraction which eluted after the main band was also collected.

Protein solutions for film voltammetry were prepared in 0.1 M NaCl, 50 mM Tris buffer solutions (pH 7.5 at room temperature) containing 200 μg/mL polymyxin sulfate as coadsorbate. Ferredoxin concentrations, as determined from visible spectra [$\epsilon = 30\ mM^{-1}\ cm^{-1}$ (*41*)], were typically ca. 100 μM. Supporting buffer electrolytes consisted of a 60 mM mixed buffer system comprising 15 mM each of MES, HEPES, TAPS, and sodium acetate, with 0.1 M NaCl and 200 μg/mL polymyxin. The pH was adjusted using concentrated NaOH or HCl solutions. Metal uptake experimental solutions contained either zinc sulfate or iron(II) ammonium sulfate as metal sources.

Protein Film Voltammetry (*39*). Analogue cyclic voltammetry was carried out using an Autolab electrochemical analyzer (Eco-Chemie, Utrecht, The Netherlands) equipped with a PGSTAT 20 or PGSTAT 30 potentiostat. The instrument supported programmable routines, in particular, the application of square pulses followed by repoising at a chosen potential and cycling over a wide dynamic range. The all-glass electrochemical cells have been described previously (*42*, *43*). The apparatus was confined within a faraday cage in order to minimize electrical noise, and a constant cell temperature of 0 °C was maintained by circulating water in the surrounding jacket. The reference electrode (SCE) was housed in a sidearm and maintained at 25 °C. All potentials quoted in this article have been adjusted to the standard hydrogen electrode (SHE) scale, with E(SHE) = E(SCE) + 241 mV at 298 K. The pyrolytic graphite edge (PGE) working electrode typically had a surface area of ca. 6 mm^2, although a smaller version was used in some fast scan rate experiments (*43*). For some control experiments, a PGE rotating-disk working electrode was used, in conjunction with an EG&G M636 electrode rotator. The counter electrode was a piece of platinum wire immersed in the same solution. For each experiment, the working electrode was polished with an aqueous alumina slurry (Buehler, 1 μm), sonicated thoroughly, and rinsed with deionized water. Protein solution was then applied to the surface with a pasteur pipet that was flame-drawn to give a fine tip. Following the sequence outlined in Figure 1, the protein film was first subjected to potential cycling (50 mV s^{-1}) over the range −0.75 to 0.1 V, the normal potential region, until a signal (B′) of stable amplitude was achieved, normally after four scans. For detailed analysis, voltammograms were corrected for nonfaradaic background current by subtracting a polynomial baseline (*44*). On the basis of the peak areas at −0.36 V, which correspond to the two [4Fe-4S] clusters with similar potentials, the average surface coverage of stable *Cp* Fd films was 33 pmol cm^{-2}, that is, close to expectations for a monolayer on a flat surface. Films could be worked for periods of up to 45 min in the normal potential region without any significant loss of coverage. However, most experiments were completed within much shorter periods (5−10 min). Once a stable film was obtained, square oxidative pulses of 0.1−5-s duration were applied at different potentials, after which cycling in the normal region was carried out to observe the changes caused by the pulse. In some cases, the potential was subsequently held for fixed periods at certain values in order to investigate the effect of locking redox centers in particular oxidation levels.

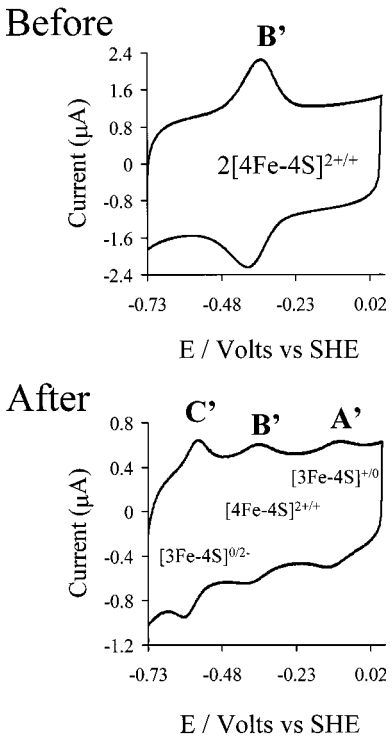

FIGURE 2: Cyclic voltammograms of *Cp* Fd adsorbed on a PGE electrode, scanned before and after applying a 3-s oxidative pulse at 0.72V (result shown is third cycle after the pulse). Voltammetry was carried out at 0 °C, scan rate 100 mV s^{-1} (before) and 50 mV s^{-1} (after). The buffer−electrolyte, pH = 5.0, contained 60 mM mixed buffer, 0.1 M NaCl, and 200 μg/mL polymyxin. The ratio of A′:B′ areas [3Fe-4S]:[4Fe-4S] after the pulse is 0.87.

Chemical Oxidation of Clusters. Chemical oxidation was carried out in a manner similar to published procedures (*26*). A solution of 8Fe ferredoxin (240 μM) was treated for 12 h at 4 °C with a 3-fold excess of potassium ferricyanide in 0.8 M NaCl, 20 mM Tris, pH 8.5, buffer. The solution was then diluted and chromatographed by FPLC. The UV/vis spectrum was shifted about 10 nm to lower energy compared to the starting material and gave an A_{400}:A_{280} ratio of 0.74. Protein film voltammetry was carried out on the products after diafiltration (Amicon YM 3 membrane).

RESULTS

Changes in Cluster Composition Following an Oxidative Pulse. Figure 2 shows cyclic voltammograms of a film of *C. pasteurianum* ferredoxin (pH = 5.0), scan rate 50 mV s^{-1}, obtained before and after application of a 3-s oxidizing pulse at 0.72 V. Initially, the 8Fe protein yields a single signal (B′) with a reduction potential of $E^{0'} = -360$ mV, which is assignable to overlapping signals from the two $[4Fe\text{-}4S]^{2+/+}$ clusters. Because intramolecular electron exchange, that is, between cluster I and cluster II, is known to be fast (*33*), it is expected that both clusters transfer electrons during the electrode process, and this was supported by experiments carried out at faster scan rates.[3] The result is consistent with results from EPR potentiometry, solution voltammetry, and NMR, which show that the reduction potentials of the two clusters differ by only 15 mV (*33*, *45*).[4]

The oxidative pulse produces two new signals in the range −0.7 to 0.1 V, while signal B′, at −360 mV, is greatly attenuated and sharpened; the average half-height width of 120 mV decreases to 104 mV. No other new signals appear. The shape of the resulting voltammogram resembles those of the 7Fe ferredoxins from *Azotobacter vinelandii*, *Desulfovibrio africanus*, and *Sulfolobus acidocaldarius*, in which the two new signals are characteristic of the [3Fe-4S] cluster (*40*). The signal at −92 mV (A′) is due to the $[3Fe\text{-}4S]^{+/0}$ redox couple, while the more intense and narrow signal (C′), with $E^{0\,\prime} = -560$ mV, corresponds to a pH-dependent cooperative two-electron process $[3Fe\text{-}4S]^{0/2-}$ associated with transfer of 2−3 H^+ (*46*).[5] Two-electron signals have not been observed for Fe−S species, other than the 3Fe cluster. The average C′:A′ area ratio is 1.9 ± 0.3, that is, close to the expected value of 2.0. Signal C′ is less well-defined at higher pH;[5] consequently, most studies were carried out at pH 5.0 to retain the clarity of this feature and, hence, provide unambiguous detection of [3Fe-4S] species. Signals A′ and C′ are the voltammetric hallmark of a [3Fe-4S] cluster, so that the area ratio of A′:B′ provides immediate and direct measurement of the 3Fe:4Fe cluster ratio in the film. We used this ratio to determine how various pulse conditions affect the different cluster populations. For the example in Figure 2, the A′:B′ ratio is 0.87, just short of the value of 1.0 expected for 7Fe ferredoxin.

A sample of protein purified by FPLC after reaction with $Fe(CN)_6^{3-}$ showed voltammetric features almost identical to those described above for the electrochemically produced species, that is, an A′:B′ ratio of 1.0 ± 0.1, as expected for the 7Fe form, although, like the electrochemical product, the chemical yield was also low (10%). Very similar voltammetry was obtained for the protein fraction which eluted as a minor band during isolation. The electrochemical pulse thus resembles the action of exposure to air or $Fe(CN)_6^{3-}$ which has a reduction potential of approximately 0.4 V vs SHE, but with the advantage of providing precise and tunable time-potential perturbations.

Dependence of [4Fe-4S] Cluster Degradation on the Pulse Potential and Pulse Duration. To establish the potential dependence of the cluster transformations, pulses of constant duration were applied at different potentials. Figure 3 shows data derived from voltammograms measured on the third cycle after 3-s pulses executed across the range 0.45−1.0 V. It is immediately evident that the population of [3Fe-4S] clusters relative to [4Fe-4S] (ratio A′:B′) maximizes at a pulse potential of approximately 0.72 V, above which the A′:B′ ratio decreases. The bell-shaped curve shows that two different processes are operating: the one at lower potential generates [3Fe-4S] clusters, while that occurring at higher potential either causes their rapid degradation or competes with their formation.

[3] Protein-film voltammetry (PFV) was carried out up to 130 V s^{-1}, the signals remaining consistent throughout, with fast electron transfer to both clusters. For further details on fast-scan PFV, see ref *43*.

[4] The reduction potentials of the two clusters in *Cp* 8Fe ferredoxin as determined by cyclic voltammetry are more positive than values obtained by other methods in which polycations are not required in order to elicit measurements. Association of polycations with the negatively charged ferredoxin enables it to adsorb at the electrode, but the favorable electrostatics also stabilize the reduced states of the clusters (see ref *45*).

[5] The magnitude of signal C′ depends dramatically on pH, because uptake of two electrons is accompanied by uptake of between two and three protons, and it disappears completely at pH values above 7.5. For further studies on the novel two-electron chemistry of [3Fe-4S] clusters, see refs *40* and *46*.

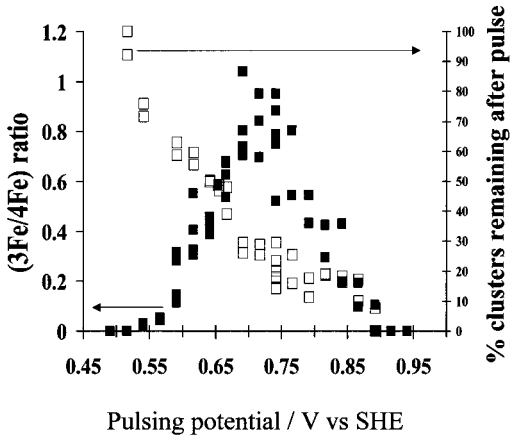

FIGURE 3: Potential dependence of the [4Fe-4S]-to-[3Fe-4S] transformation. The black squares show the ratio [3Fe-4S]:[4Fe-4S] as measured from the third cycle following a 3-s pulse at the stated potential values. The open squares represent the total cluster population observed after the pulse. This is represented as a percentage, that is, $100[(A' + B')/B_0']$, where A′ and B′ are the areas of the corresponding signals after the pulse, and B_0' is the area of the signal before the pulse. Other conditions were as given in the legend to Figure 2.

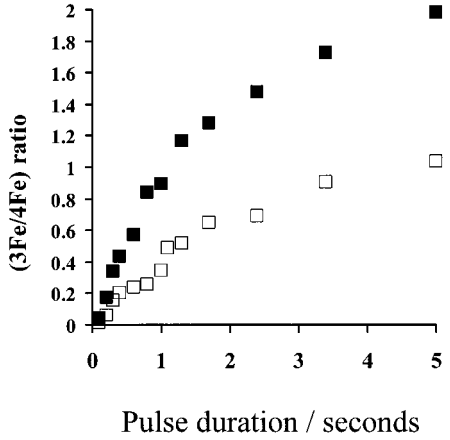

FIGURE 4: Time dependence of cluster transformations following an oxidative pulse. In this case the protein film was exposed to 0.69-V pulses of different duration. Other conditions were as given in the legend to Figure 2. The plot shows the ratio of [3Fe-4S] clusters to [4Fe-4S] clusters measured in the first (■) and third (□) cyclic voltammograms after the pulse.

Figure 3 also shows how the total cluster population, expressed as a percentage relative to the initial [4Fe-4S] population, decreases with increasing pulse potential. Complete loss of signals occurs almost entirely within the limits of the bell-shaped potential curve for [3Fe-4S] generation. This may be due either to loss of both clusters or to protein desorption; but the fact that signals due to [4Fe-4S] clusters persist at the higher potentials, beyond which [3Fe-4S] products are difficult to observe, shows that a significant number of protein molecules are still bound to the electrode.[6]

Figure 4 shows the effect of varying the pulse duration at a fixed potential (0.69 V), from which it is clear that the 3Fe:4Fe ratio approaches a limiting value. There is also a marked difference between ratios obtained from the first and third cycles; in particular, for a 5-s pulse, the first reveals a significant excess of [3Fe-4S] clusters, whereas the third shows a ratio close to unity.

[6] It is difficult to assess independently the degree to which desorption may be induced by the oxidative pulse or whether proteins having one cluster type are more easily lost than ones with another type or indeed with both clusters lost. Changes in capacitance are not helpful or reliable because the graphite surface itself is altered by oxidation.

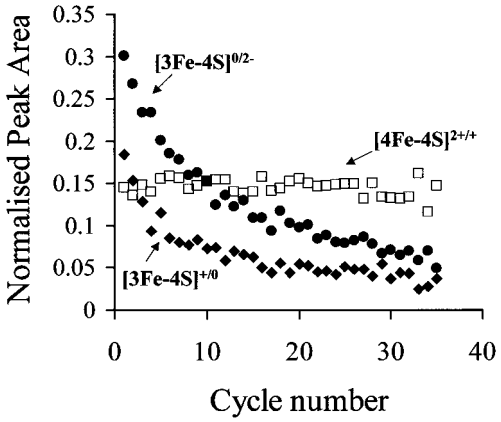

FIGURE 5: Normalized signal areas (measured using oxidative peaks) for successive cyclic voltammograms recorded after a 3-s pulse at 0.72 V. Other conditions were as given in the legend to Figure 2. Black markers represent [3Fe-4S] cluster signals (● = A′, $[3Fe\text{-}4S]^{+/0}$; ◆ = C′, $[3Fe\text{-}4S]^{0/2-}$) and the open squares represent signal B′ ($[4Fe\text{-}4S]^{2+/+}$). Clearly, the [3Fe-4S] cluster undergoes further degradation, while the [4Fe-4S] cluster population remains stable.

Subsequent Reactions of [3Fe-4S] Products. The experiments described so far show that conditions can be fine-tuned to optimize formation of [3Fe-4S] clusters in an otherwise complex system. The next step was to study the subsequent fates of the [3Fe-4S] products under various conditions. Figure 5 shows how the peak areas A′, B′, and C′, from continuous cyclic voltammograms scanned in the normal region at 50 mV s^{-1}, change after a 3-s pulse at 0.72 V. The areas have been normalized with respect to the magnitude observed before the pulse and reflect the overall losses evident in Figure 3. The remaining signals display systemmatic changes, the most significant being that the [3Fe-4S] clusters degrade further (the A′ and C′ signal intensities decrease in parallel) over a time period during which signal B′, due to [4Fe-4S] clusters, remains constant.

The disappearance of [3Fe-4S] clusters which occurs after reducing conditions have been restored was clarified by further experiments in which, instead of cycling, the initial oxidative pulse was followed by periods in which the potential was held at values specifically favoring each oxidation level (0.06 V, $[3Fe\text{-}4S]^{+}$; −0.21 V, $[3Fe\text{-}4S]^{0}$; and −0.73 V, $[3Fe\text{-}4S]^{2-}$). At each interval, the cluster status was ascertained from a single cyclic voltammogram conducted at 0.5 V s^{-1}, which is sufficiently fast to minimize reactions during passage. Figure 6 shows the ratios A′:B′, that is, [3Fe-4S]:[4Fe-4S], measured as a function of time for the three potential values.

The results suggest that the hyper-reduced cluster $[3Fe\text{-}4S]^{2-}$ is labile in *Cp* Fd and must be largely responsible for the rapid breakdown of [3Fe-4S] clusters, as monitored by potential cycling.[7] Indeed, once this pathway is blocked, by holding the potential to lock [3Fe-4S] products in the + and 0 oxidation levels, it emerges that a significant excess population of [3Fe-4S] is present immediately after the oxidative pulse. In all cases, the [3Fe-4S]:[4Fe-4S] ratio falls rapidly, but for $[3Fe\text{-}4S]^{+}$, it stabilizes around 1.0, a result

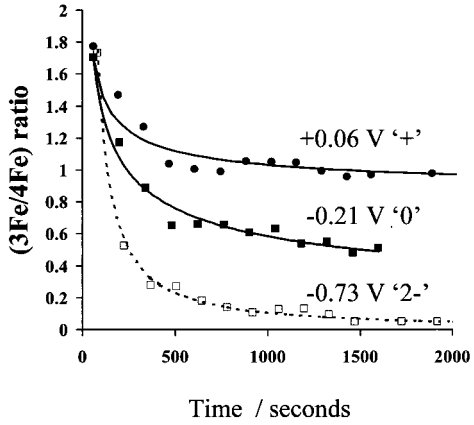

FIGURE 6: Variation with time of the [3Fe-4S]:[4Fe-4S] cluster ratio after a 3-s pulse at 0.72 V and subsequently holding the electrode potential at values locking each of the different oxidation levels of the [3Fe-4S] cluster. Other conditions were as given in the legend to Figure 2. Black circles show data obtained when the potential was held at 0.061 V (+); black squares, −0.209 V (0); open squares, −0.734 V (2−).

fully consistent with formation of a relatively stable 7Fe protein, as concluded by Bertini and co-workers (*26*). In Figure 7, the data are shown in terms of peak areas for [3Fe-4S] and [4Fe-4S], normalized with respect to the prepulse area, rather than as a ratio. It is now evident that provided the labile 2− state is avoided, the initial loss of [3Fe-4S] cluster that occurs after restoring normal potentials is accompanied by a proportionate increase in [4Fe-4S]. Also shown in Figure 7 are data obtained in the presence of EGTA (5 mM), which is a mild sequestering agent for Fe(II) and has no effect on the voltammetry of the 8Fe form prior to the pulse. While EGTA serves generally to accelerate cluster degradation after the pulse, careful inspection reveals that there is also a significant dependence on the [3Fe-4S] oxidation level. For the + level, EGTA produces rapid loss of the initial excess of [3Fe-4S] without a corresponding recovery of [4Fe-4S], whereas for the 0 level, a loss of excess [3Fe-4S] occurs in parallel with the recovery of [4Fe-4S] clusters and at a rate similar to that of the zero-EGTA experiment.

Reversibility. It is well-known that [3Fe-4S] clusters in several ferredoxins (*Desulfovibrio gigas, Pyrococcus furiosus,* and *D. africanus*) take up metal ions M from solution to form cubanes of the type [M3Fe-4S] (*30, 31, 36, 47, 48*). This process occurs reversibly between the states $[3Fe\text{-}4S]^0$ and $[M3Fe\text{-}4S]^{2+}$ (*30*). To test whether the [3Fe-4S] products of *Cp* Fd oxidative degradation are similarly active, we carried out experiments in the presence of metal ions. Figure 8 shows the result obtained after applying a 3-s pulse at 0.72 V and transferring the electrode to a cell containing Fe^{2+} (30 mM).[8] The potential was then held at −210 mV to lock the $[3Fe\text{-}4S]^0$ state and was cycled periodically at 500 mV s^{-1} to quantify the clusters. Although the normalized [3Fe-4S] population, that is, with respect to the initial number of

[7] An alternative explanation would require that negative potentials induce selective desorption of protein molecules containing only [3Fe-4S] clusters. This must be considered much less likely in view of the fact that EGTA exerts a significant effect on the loss of signals. Electrostatics also stabilizes the reduced states of the clusters. See ref *45*.

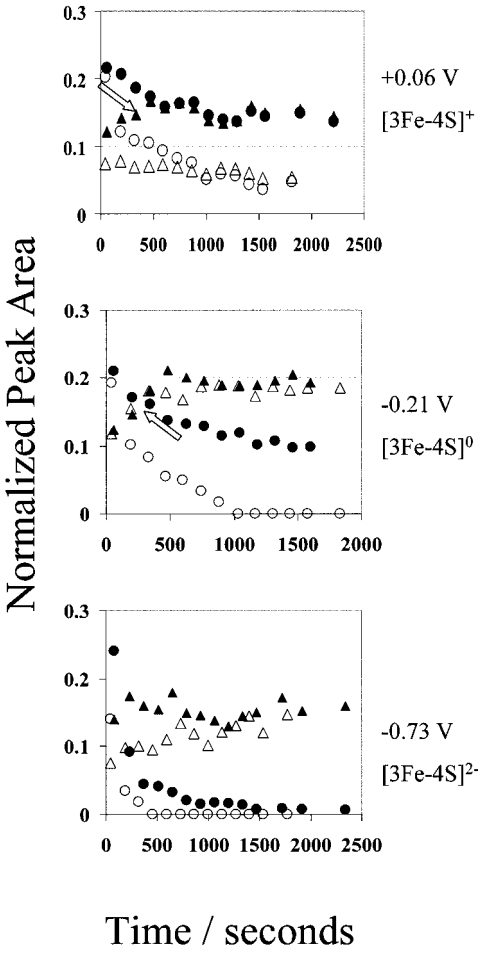

FIGURE 7: Data from the same experiment depicted in Figure 6 and from a similar experiment carried out in the presence of EGTA in which the actual peak areas associated with [3Fe-4S] and [4Fe-4S] clusters, normalized to the starting 8Fe sample, are plotted. The [3Fe-4S] cluster population is represented by circles and the [4Fe-4S] population by triangles. Solid and open markers represent, respectively, data obtained in the absence or presence of EGTA (5 mM). Block arrows indicate where initial increases in [4Fe-4S] population occur after the pulse.

[4Fe-4S] clusters, was initially 0.1, signals A′ and C′ disappeared completely over 20 min, while B′ increased in area to give a stable product which, apart from the lower amplitude, was electrochemically indistinguishable from the 8Fe protein present before the pulse.

A novel opportunity to probe the species formed during the pulse was afforded by carrying out the experiment in the presence of Zn^{2+}. First, because Zn^{2+} is redox inactive, it can be present in situ during the pulse to trap any highly reactive [3Fe-4S] clusters. Second, signals due to $[Zn3Fe\text{-}4S]^{2+/+}$ products should be distinguishable from the surviving $[4Fe\text{-}4S]^{2+/+}$ clusters by virtue of their different reduction potentials. Figure 9 shows a sequence of voltammograms scanned at 6 V s^{-1} after pulsing a film of 8Fe *Cp* Fd for 3 s at 0.72 V in a solution containing 11 mM Zn^{2+}. Every fifth cycle is displayed, and from the disappearance of signals A′ and C′, it is immediately evident that the [3Fe-4S] clusters formed during the pulse react rapidly with Zn. In their place,

[8] Oxidative pulses carried out in the presence of Fe^{2+} generate Fe(III) species that obscure the signals of Fe−S clusters in subsequent voltammetric cycles.

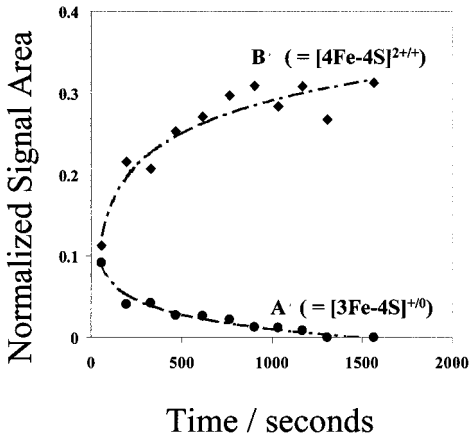

FIGURE 8: Uptake of Fe^{2+} by the products of cluster disassembly generated using a 3-s pulse at 0.72 V. After pulsing, the electrode was transferred to buffer−electrolyte containing 30 mM Fe^{2+}, the electrode potential was held at −209 mV, and scans were recorded approximately every 2 min. Other conditions were as given in the legend to Figure 2. Note that the 4Fe signal B′ (◆) increases by a greater amount than that by which the 3Fe signal A′ (●) decreases.

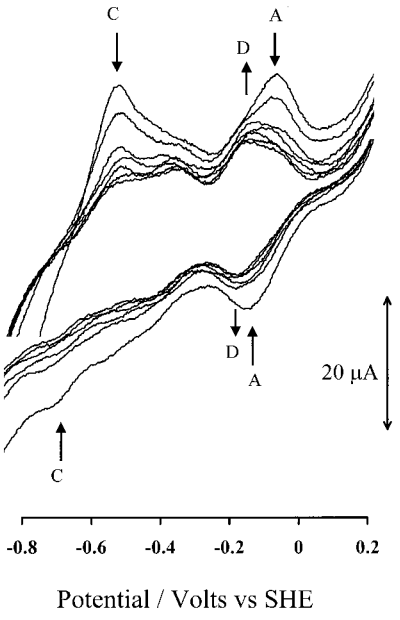

FIGURE 9: Voltammograms following a 3-s pulse at 0.72 V carried out in the presence of Zn^{2+} (11 mM) at 0 °C. The voltammetric scan rate was 6 V s^{-1}; other conditions were as given in the legend to Figure 2. Every fifth cycle is shown. For clarity, most of the capacitance component has been removed. Arrows indicate direction of change of signals.

a new signal, D′, appears ($E^{0\prime}$, approximately −160 mV) which, on the basis of the results for other Fe−S systems, can be assigned to $[Zn3Fe\text{-}4S]^{2+/+}$(*30*, *31*, *36a*, *48b*). The new species now accounts for at least 50% of the cluster population of the sample. Analysis of the time dependence shows that this transformation occurs in at least two phases. For example, even by the second cycle, the new signal already represents 30% of the total new-signal amplitude, and reaction is still proceeding after 30 s. The products are stable in their reduced state, $[Zn3Fe\text{-}4S]^{+}$, but reversion to [3Fe-4S] is almost complete after 10 s if the potential is held at 60 mV, which locks all the [Zn3Fe-4S] clusters in the 2+ level. Although the analysis shows an excess of Zn adducts, suggesting that many protein molecules must contain two

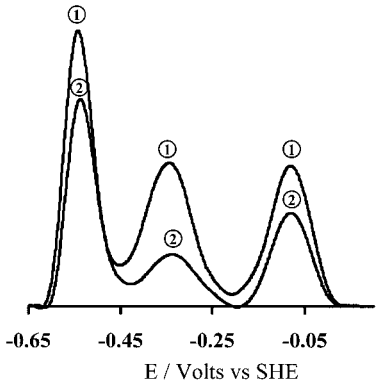

FIGURE 10: Double-pulse experiments conducted to compare oxidative degradation of [3Fe-4S] and [4Fe-4S] clusters. Figure shows the baseline-subtracted voltammograms (oxidation direction) corresponding to a double-pulse sequence. (1) Product of the first pulse (0.72 V, 3 s) after poising 4 min at 60 mV to establish 7Fe protein; (2) product of the second pulse (0.72 V, 3s) applied to the 7Fe protein. Other conditions were as given in the legend to Figure 2.

[Zn3Fe-4S] clusters, there was no noticeable broadening to indicate any significant difference in their reduction potentials, as is also the case for molecules containing two [3Fe-4S] or two [4Fe-4S] clusters.

Double-Pulse Experiments. To determine why formation of [3Fe-4S] clusters does not occur at very high potentials (referring to the right-hand side of the bell-shaped plot in Figure 3), a double-pulse sequence was utilized. This involved applying a primary oxidative square pulse to obtain the 7Fe form, then applying a second pulse to test how the [3Fe-4S] and [4Fe-4S] clusters are differentially affected. Results are shown in Figure 10. As expected, the first pulse produced a small excess of [3Fe-4S] clusters over [4Fe-4S], following which the excess was removed, yielding 7Fe protein, by holding the potential at 60 mV for 4 min. The second pulse triggered further overall loss of signals, down to 49% of that observed after the first pulse, but the ratio of 3Fe to 4Fe increased to 1.4 (42% B′ and 58% A′). Thus, [3Fe-4S] clusters are relatively resistant to oxidation and, indeed, are probably formed at the expense of the remaining population of [4Fe-4S].

Square-Wave Voltammetry. Cyclic voltammetry on 8Fe ferredoxin films in the high-potential region accessed during oxidative pulses did not reveal any reversible signals that might be attributable to the $[4Fe\text{-}4S]^{3+/2+}$ couple; only a large broad oxidative wave was observed around 0.7 V. Therefore, further checks were made using square-wave voltammetry. As shown in Figure 11, this technique revealed two overlapping peaks, with apparent potentials of approximately 690 and 822 mV.

DISCUSSION

These experiments have exploited the ability to trigger potential-dependent cluster transformations under precise potential control, to identify unambiguously and quantify [3Fe-4S] species as they are formed during the oxidative disassembly of [4Fe-4S] clusters, and, hence, to evaluate how these clusters might yield to thermodynamic pressures imposed, even for short periods, within the biological environment. Each of the two clusters present in *Cp* Fd has the classical cluster binding sequence and all-cysteine ligation

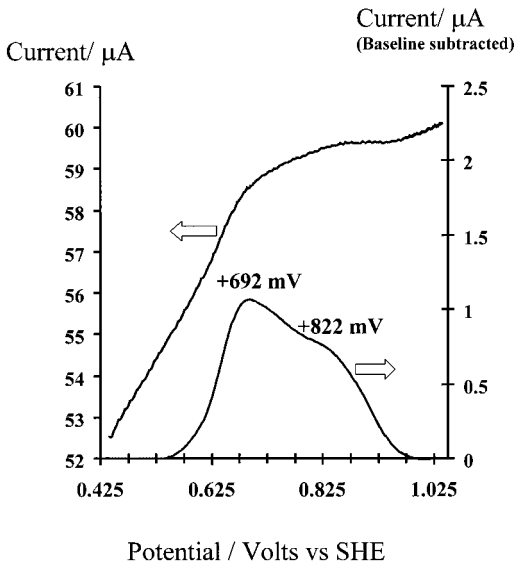

FIGURE 11: Square-wave voltammetry of 8Fe *Cp* Fd. Raw data and an enhanced plot obtained by baseline correction. Amplitude, 50 mV; frequency, 50 Hz; and step potential, 3 mV, commencing from lower potential limit. Other conditions were as given in the legend to Figure 2.

that are typical of the great majority of [4Fe-4S] clusters so far characterized, so that the results are likely to have quite general relevance.

Both the original [4Fe-4S] and generated [3Fe-4S] clusters in this small protein (molecular mass ca. 6 kDa) show fast electron transfer, so it is unlikely that other discrete cluster species that might be formed would be electrochemically silent and go undetected. Although generation of other species, for example, [2Fe-2S] clusters, cannot be completely ruled out, these have not been detected in chemical oxidation experiments with this protein (*25, 26*), and no new signals apart from those characteristic of [3Fe-4S] are observed after applying pulses across a wide potential range. Complete loss of electrochemical activity occurs across the range of the bell-shaped potential profile defining formation of [3Fe-4S] species, and the observation that this loss is accelerated in the presence of EGTA suggests strongly that in addition to loss from desorption, there is total cluster disassembly and formation of apoprotein. Referencing the [3Fe-4S] cluster population to that of the remaining [4Fe-4S] clusters largely overcomes the problem of needing to gauge how much protein is lost by desorption. The transformations are to some extent reversible, even when the electrode is rotating rapidly, which disperses desorbed protein. The overwhelming evidence is that a brief oxidative pulse above 0.5 V triggers very rapid degradation of the 8Fe ferredoxin, that is, within a few seconds, and the reaction proceeds to clusterless forms, although significant yields of [3Fe-4S] cluster are obtained by fine-tuning the potential and duration of the pulse. The persistence, shortly after the pulse, of a stable 7Fe protein is fully consistent with the NMR experiments carried out by Bertini and co-workers (*26*), and the results will be discussed henceforth in terms of the events depicted in Scheme 2.

Application of a pulse at a potential <0.72 V initially produces an excess of [3Fe-4S] clusters over [4Fe-4S]; however, the excess population is much more reactive, and after the pulse there is a rapid transition to a voltammogram characteristic of a 7Fe ferredoxin. This product may be identified with that assigned by Bertini and co-workers in which the cluster isolated in its 3Fe form is denoted cluster I (*26*). Thus, a 6Fe protein is generated, in which the second [3Fe-4S] cluster sequesters Fe very efficiently to rebuild a [4Fe-4S] center. The fact that both of the [3Fe-4S] clusters must have indistinguishable reduction potentials is not surprising, given the similarity of values for the two [4Fe-4S] clusters in the 8Fe protein. The Fe may originate from trace levels in solution or perhaps from Fe that has somehow remained bound to the protein but cannot be detected electrochemically as a discrete species. The affinity is very high, and only if the [3Fe-4S] cluster is held in the + level does EGTA prevent reformation of [4Fe-4S].

The increase in signal B′ and decrease in signals A′ and C′ that are observed when the electrode is transferred after the pulse to a solution of Fe^{2+} show that the [3Fe-4S] cluster in the 7Fe protein can also be transformed easily back to [4Fe-4S]. The fact that the observed increase, equivalent to 0.3 of the original cluster population, is considerably higher than the corresponding disappearance of [3Fe-4S] clusters (0.1) suggests that some [4Fe-4S] clusters are also regenerated from apo sites (i.e., lacking at least Fe). The high reactivities of the [3Fe-4S] clusters formed by the pulse are confirmed by experiments in which the pulse is executed in the presence of Zn^{2+}. Replacement of signal A′ due to $[3Fe\text{-}4S]^{+/0}$ by a new signal attributable to $[Zn3Fe\text{-}4S]^{2+/+}$ occurs in two stages. Much of the reaction is complete within a few seconds, while the remainder transforms within a minute. A likely reason for the biphasic kinetics is that the two [3Fe-4S] clusters have different rates of Zn^{2+} binding. The observation that reactions with Zn^{2+} are faster than with Fe^{2+} is expected on the basis of their respective intrinsic inner-sphere ligand-exchange rates (*49*). However, Zn is less tightly bound and readily dissociates from the oxidized $[Zn3Fe\text{-}4S]^{2+}$ cluster.

The time and potential dependences of cluster breakdown and the appearance of [3Fe-4S] clusters can be discussed within the framework of Scheme 3.

The fact that the potential required to form [3Fe-4S] clusters is much higher than the reduction potentials of the resulting products, the $[3Fe\text{-}4S]^{+/0}$ cluster and Fe(III):(II) solution species, shows that Fe release does not depend merely on trapping the products, that is, because the [3Fe-4S] cluster has little affinity for a fourth Fe when in the + level. This is in contrast to the situation found for the labile [4Fe-4S] cluster in ferredoxin III from *D. africanus*, in which the Fe is loosely bound and can be removed from the O-ligated subsite, aspartate carboxylate or possibly HO(H), simply by trapping the [3Fe-4S] product in the + state (*30*). Rather, the rate-determining process involves further oxidation of $[4Fe\text{-}4S]^{2+}$. Indeed, the data (vide infra) show this is a one-electron process, thus producing a species at the 3+ level. Application of pulsing potentials below E_1 restricts the reaction more to that shown inside the broken-line box in Scheme 3, that is, generation of the [3Fe-4S] cluster, whereas higher-pulsing potentials activate more extensive cluster destruction. Two possibilities for the second potential-dependent process are (A) a competing process in which the immediate product $[4Fe\text{-}4S]^{3+}$ is oxidized further to a very reactive product which undergoes rapid, irreversible degradation to redox-inactive products and (B) a sequential process in which the $[3Fe\text{-}4S]^{+}$ degradation product undergoes further

Scheme 2: Various Potential-Dependent Transformations of the Two Clusters, I and II, in *Cp* Fd That Are Revealed by the Voltammetric Pulse Experiments

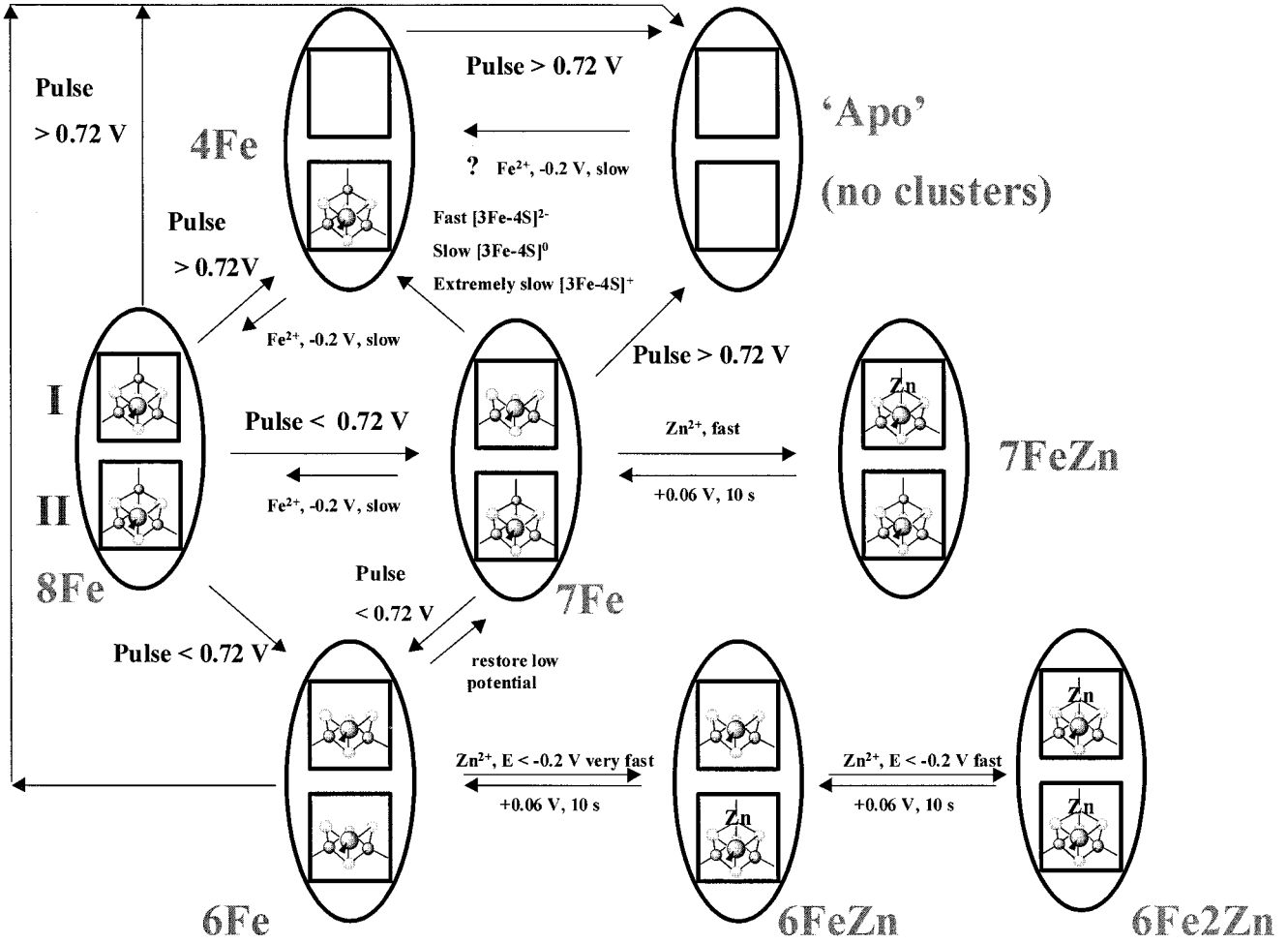

Scheme 3: Oxidative Disassembly of [4Fe-4S] Clusters via the 3+ Oxidation Level[a]

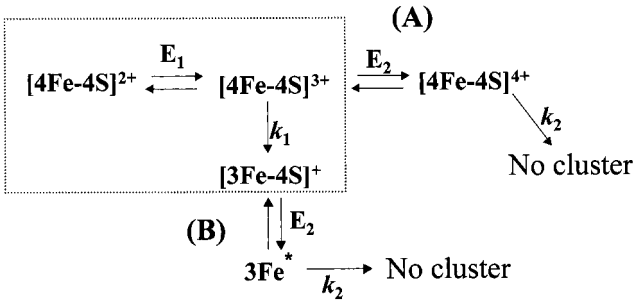

[a] The relative resilience of [3Fe-4S] to further oxidative breakdown suggests that complete disassembly of [4Fe-4S] clusters proceeds via pathway A.

oxidation, most likely at S atoms, to a species that decomposes irreversibly, again giving redox-inactive products. That A is the preferred pathway can be concluded from the results of the double-pulse experiment (Figure 10), which confirm that [3Fe-4S] is more resilient to oxidation than [4Fe-4S]. The decrease in signal A′ that occurs on the second pulse seems likely instead to reflect the extent of protein desorption that occurs as the electrode potential is made very positive.

Numerical analysis was carried out in terms of Scheme 3, that is, two consecutive one-electron processes, with the intermediate either releasing Fe to produce a stable species or undergoing further oxidation to initiate catastrophic breakdown. The analysis was simplified by assuming that only a single [3Fe-4S] product is being measured. The results and fits obtained are shown in Figures 12 and 13; the two data sets in each case correspond to values taken from first or third cycles.[9] Despite the simplification, excellent fits are obtained for the time dependence and (although less well-fitted) for the bell-shaped potential curve. Only a narrow range of rate constants gave acceptable agreement, and no satisfactory fits could be made on the basis of cooperative two-electron processes.

The results show that degradation is initiated by a one-electron oxidation of $[4Fe\text{-}4S]^{2+}$ at reduction potential E_1

[9] Digital simulation of the data shown in Figures 4 and 5 utilized a finite difference method, with convergence being achieved with time step sizes of 10^{-6} s. Some simplifying assumptions were required, a major one being that the formation of [3Fe-4S] is largely restricted to just one cluster. This was justified becasue one of these, denoted cluster I, is retained in the 3Fe form much more readily than cluster II, which reverts rapidly back to a [4Fe-4S] cubane. From Figures 5−7, it can be seen that the initial excess of [3Fe-4S], which is produced immediately after the pulse, is removed after the second cycle, during which the 3Fe:4Fe ratio adjusts to approximately 1:1. The third cycle thus essentially records only the more stable [3Fe-4S] cluster. As an alternative, the first scans after the pulse were analyzed, applying a cutoff in which any higher 3Fe:4Fe ratio is considered as 1.0. Comparison between the two methods can be seen in Figures 12 and 13. The results are qualitatively similar, and the quantitative agreement is acceptable, given the inherent error margins.

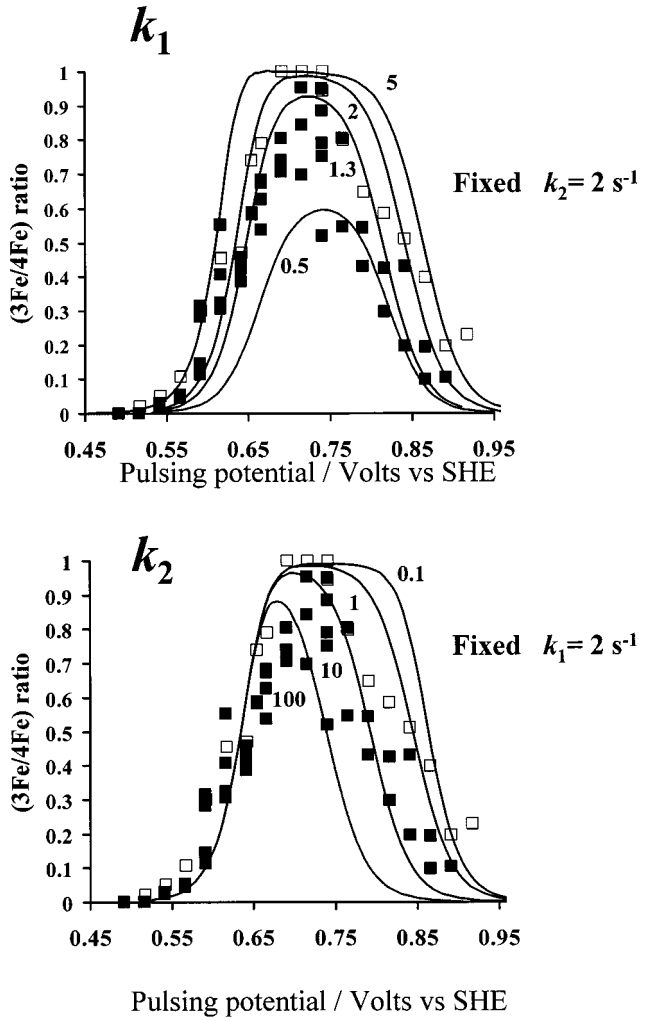

FIGURE 12: Modeling of the pulse-potential dependence, in which data from first (■) and third (□) scans are compared. Data were taken from experiments with conditions as given in the legend to Figure 2. Lines correspond to the calculations performed according to Scheme 3 (pathway A: $E_1 = 670$ mV, $E_2 = 830$ mV). The upper chart shows the effect of varying k_1 while k_2 is held constant, and the lower chart shows the effect of varying k_2 while k_1 is held constant.

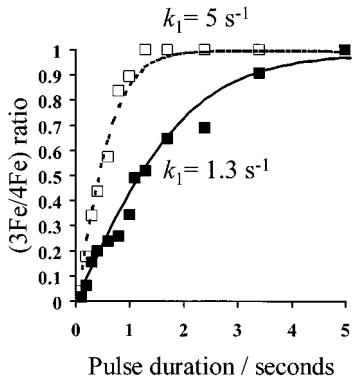

FIGURE 13: Modeling of the pulse-duration dependence, according to Scheme 3 (path A: $E_1 = 670$ mV, $E_2 = 830$ mV). Data were taken from experiments with conditions as given in the legend to Figure 2. Using first scans, □, with k_1= 5 s^{-1}; or using third scans, ■, with $k_1 = 1.3$ s^{-1}.

and requires that the product, formally [4Fe-4S]$^{3+}$, then either expels an Fe with a rate constant of ca. 1 s^{-1} or undergoes further oxidation, reduction potential E_2, which triggers rapid and much more extensive damage. The one-electron characteristic of E_2 suggests that the short-lived product is [4Fe-4S]$^{4+}$, that is, formally an all-Fe(III) cluster which has never before been detected, although at the more detailed level, S-based oxidation cannot be ruled out. The rate constant for the second process is less well-defined (k_2 lies nearer to 10 s^{-1}), but the comparable-or-higher rate of decay and higher reduction potential mean that the short-lived product would probably evade detection in a conventional experiment. The two reduction potentials defined by the bell-shaped curve agree quite well with those observed by square-wave voltammetry (692 and 822 mV).[10] As is known for other redox couples of Fe−S clusters, the potential required to access the iron-releasing [4Fe-4S]$^{3+}$ state is likely to depend significantly on protein tertiary structure and solvent accessibility (*20*). To address this issue, we are currently extending the methodology here presented to a wide variety of 4Fe centers in different proteins.

The subsequent reactions which occur after returning to normal potentials are relevant in that oxidative stress in biology might, like the electrochemical pulse, be of short duration. The [3Fe-4S] clusters that emerge from the pulse vary in their activities. The more reactive one, cluster II, is rapidly repaired, while the behavior of the more inert one, cluster I, reveals that further breakdown requires a reducing environment and an absence of Fe in the immediate environment. Under physiological conditions, the [3Fe-4S] cluster is likely to persist in the + or 0 oxidation levels, rather than the very reducing 2− state which is labile in this protein. The + level is stable but has only a low affinity for Fe(II). The 0 state undergoes slow degradation, but in the presence of Fe(II), the [4Fe-4S] cluster is recovered.

In conclusion, these experiments yield a quantitative model for the response of Fe−S clusters to oxidative stress that might be mediated by a burst of reactive species. Rapid oxidative disassembly of the two [4Fe-4S] clusters of *C. pasteurianum* 8Fe ferredoxin proceeds rapidly upon application of potentials above 0.6 V. Importantly, the experiments show that the [3Fe-4S] clusters which appear are not intermediates on a linear pathway to apoprotein but rather are formed if Fe is released before a second electron is removed; that is, they represent relatively safe havens that are resistant to further oxidative disassembly. Both of the [4Fe-4S] clusters in the protein can be converted to [3Fe-4S] forms, but these products have different reactivities, and one is rapidly repaired even if no additional Fe is present. Significantly, it is the restoration of reducing conditions which provides the pathway for further disassembly of [3Fe-4S]; thus, the [3Fe-4S] cluster in the 7Fe protein is retained if it is locked in the + oxidation level but breaks down upon reduction to the 0 or, particularly, the 2− level. However, at the 0 level, Fe^{2+} or indeed Zn^{2+} can stabilize the cluster by binding to reform a cubane. The observation that Fe(II) binds more tightly than Zn(II) shows the importance of resonance stabilization (*50*). The reversibility of [4Fe-4S] disassembly as far as [3Fe-4S] is, therefore, confirmed for a

[10] Square-wave voltammetry produces better resolution of two or more redox processes that have quite similar reduction potentials. The chemically irreversible nature of the reactions probably accounts for the poor agreement with values (0.79, 1.12 V) determined earlier by differential-pulse voltammetry on ferredoxin solutions (pH 7) in the presence of Mg^{2+}.

system having all-cysteine ligation. Provided electron transfer between clusters and electrode is fast, the PFV method enables a remarkable number of manipulations to be carried out under precise conditions, and any such application to the larger and more complex systems of known biological relevance may significantly improve our understanding of how the status of Fe−S clusters is controlled in proteins.

ACKNOWLEDGMENT

We thank Dr. Dirk Heering for his helpful suggestions. R. Camba thanks the National Council of Science and Technology of Mexico (CONACYT) for their support.

REFERENCES

1. Beinert, H., Holm, R. H., and Münck, E. (1997) *Science 277*, 653−659.
2. Johnson, M. K. (1998) *Curr. Opin. Chem. Biol. 2*, 173−181.
3. Flint, D. H., and Allen, R. M. (1996) *Chem. Rev. 96*, 2315−2334.
4. Cammack, R., and Sykes, A. G., Eds. (1999) *Advances in Inorganic Chemistry*, Vol. 47, Academic Press, New York.
5. Peters, J. W., Lanzilotta, W. N., Lemon, B. J., and Seefeldt, L. C. (1998) *Science 282*, 1853−1858. Lancaster, C. R. D., Kröger, A., Auer, M., and Michel, H. (1999) *Nature 402*, 377−385.
6. Hirst, J., Duff, J. L. C., Jameson, G. N. L., Kemper, M. A., Burgess, B. K., and Armstrong, F. A. (1998) *J. Am. Chem. Soc. 120*, 7085−7094. Lanzilotta, W. N., Christiansen, J., Dean, D. R., and Seefeldt, L. C. (1998) *Biochemistry 37*, 11376−11384.
7. Schindelin, N., Kisker, C., Sehlessman, J. L., Howard, J. B., and Rees, D. C. (1997) *Nature 387*, 370−376.
8. Lieder, K. W., Booker, S., Ruzicka, F. K., Beinert, H., Reed, G. H., and Frey, P. A. (1998) *Biochemistry 37*, 2578−2585. Staples, C. R., Ameyibor, E., Fu, W., Gardet-Salvi, L., Strit-Etter, A., Schürmann, P., Knaff, D. B., and Johnson, M. K. (1996) *Biochemistry 35*, 11425−11434. Külzer, R., Pils, T., Kappl, R., Hüttermann, J., and Knappe, J. (1998) *J. Biol. Chem. 273*, 4897−4903.
9. Duin, E., Lafferty, M. E., Crouse, B. R., Allen, R. M., Sanyal, I., Flint, D. H., and Johnson, M. K. (1997) *Biochemistry 36*, 11811−11820.
10. Beinert, H., Kennedy, M. C., and Stout, C. D. (1996) *Chem. Rev. 96*, 2335−2373.
11. Beinert, H., and Kiley, P. J. (1996) *FEBS Lett. 382*, 218−219. Paraskeva, E., and Hentze, M. (1996) *FEBS Lett. 389*, 40−43. Schalinske, K. L., Anderson, S. A., Polygena, T. T., Chen, S. O., Kennedy, M. C., and Eisenstein, R. S. (1997) *Biochemistry 36*, 3950−3958. Pantopoulos, K., and Hentze, M. (1998) *Proc. Natl. Acad. Sci. U.S.A. 95*, 10559−10563. Beinert, H., and Kiley, P. J. (1999) *Curr. Opin. Chem. Biol. 3*, 152−157. Alén, C., and Sonenshein, A. L. (1999) *Proc. Natl. Acad. Sci. U.S.A. 96*, 10412−10417.
12. Gardner, P., Raineri, I., Epstein, L. B., and White, C. W. (1995) *J. Biol. Chem. 270*, 13399−13405. Yan, L., Levine, R., and Sohal, R. S. (1997) *Proc. Natl. Acad. Sci. U.S.A. 94*, 11168−11172. Keyer, K., and Imlay, J. A. (1997) *J. Biol. Chem. 272*, 27652−27659.
13. Gardner, P., and Fridovich, I. (1991) *J. Biol. Chem. 266*, 1478−1483.
14. Flint, D. H., Tuminello, J. F., and Emptage, M. H. (1993) *J. Biol. Chem. 268*, 22369−22376. Flint, D., Smyk-Randall, E., Tuminello, J., Draczynska-Lusiak, B., and Brown, O. R. (1993) *J. Biol. Chem. 268*, 25547−25552. Brown, O. R., Smyk-Randall, E., Draczynska-Lusiak, B., and Fee, J. A. (1995) *Arch. Biochem. Biophys. 319*, 10−22.
15. Smith, J. L., Zaluzec, E. J., Wery, J.-P., Niu, L., Switzer, R. L., Zalkin, H., and Satow, Y. (1994) *Science 264*, 1427−1433.
16. Iwai, K., Drake, S. K., Wehr, N. B., Weissman, A. M., LaVaute, T., Minato, N., Klausner, R. D., Levine, R. L., and Rouault, T. A. (1998) *Proc. Natl. Acad. Sci. U.S.A. 95*, 4924−4928. Pantopoulos, K., and Hentze, M. (1995) *EMBO J. 14*, 2917−2924. Pantopoulos, K., Mueller, S., Atzberger, A., Ansorge, W., Stremmel, W., and Hentze, M. (1997) *J. Biol. Chem. 272*, 9802−9808.
17. Khoroshilova, N., Popescu, C., Münck, E., Beinert, H., and Kiley, P. (1997) *Proc. Natl. Acad. U.S.A. 94*, 6087−6092. Popescu, C. V., Bates, D. M., Beinert, H., Münck, E., and Kiley, P. J. (1998) *Proc. Natl. Acad. U.S.A. 95*, 13431−13435. Lazazzera, B. A., Beinert, H., Khoroshilova, N., Kennedy, M. C., and Kiley, P. (1996) *J. Biol. Chem. 271*, 2762−2768.
18. Ding, H., and Demple, B. (1998) *Biochemistry 37*, 17280−17286. Hidalgo, E., Ding, H., and Demple, B. (1997) *Cell 88*, 121−129. Gaudu, P., Moon, N., and Weiss, B. (1997) *J. Biol. Chem. 272*, 5082−5086.
19. Cotton, F. A., Murillo, C., Wilkinson, G., Bochmann, M., and Grimes, R. (1999) *Advanced Inorganic Chemistry*, p 788, John Wiley and Sons, Inc., New York.
20. Stephens, P. J., Jollie, D. R., and Warshel, A. (1996) *Chem. Rev. 96*, 2491−2513.
21. Mayerle, J. J., Denmark, S. E., DePamphilis, B. V., Ibers, J. A., and Holm, R. H. (1975) *J. Am. Chem. Soc. 97*, 1032−1045. Cambray, J., Lane, R. W., Wedd, A. G., Johnson, R. W., and Holm, R. H. (*1977*) *Inorg. Chem. 16*, 2565−2571.
22. Huie, R. E., and Neta, P. in *Reactive Oxygen Species in Biological Systems* (Gilbert, D. L., and Colton, C. A., Eds) Kluwer Academic/Plenum Publishers, New York.
23. Bertini, I., Gray, H. B., Lippard, S. J., and Valentine, J. S. (1994) *Bioinorganic Chemistry*, University Science Books, Mill Valley, CA.
24. Imlay, J. A., and Linn, S. (1988) *Science 240*, 1302−1309. Keyer, K., Gort, A. S., and Imlay, J. A. (1995) *J. Bacteriol. 177*, 6782−6790. Storz, G., Imlay, and J. A. (1999) *Curr. Opin. Microbiol. 2*, 188−194.
25. Thomson, A. J., Robinson, E. A., Johnson, M. K., Cammack, R., Rao, K. K., and Hall, D. O. (1981) *Biochim. Biophys. Acta 637*, 423−432. Johnson, M. K., Spiro, T. G., and Mortenson, L. E. (1982) *J. Biol. Chem. 257*, 2447−2452.
26. Bertini, I., Briganti, F., Calzolai, L., Messori, L., and Scozzafava, A. (1993) *FEBS Lett. 332*, 268−272.
27. Moura, J. J. G., Moura, I., Kent, T. A., Lipscomb, J. D., Hanh-Huynh, B., LeGall, J., Xavier, A., and Münck, E. (1982) *J. Biol. Chem. 257*, 6259−6267.
28. Conover, R. C., Kowal, A. T., Fu, W., Park, J.-B., Aono, A., Adams, M. W. W., and Johnson, M. K. (1990) *J. Biol. Chem. 265*, 8533−8541.
29. George, S. J., Armstrong, F. A., Hatchikian, E. C., and Thomson, A. J. (1989) *Biochem. J. 264*, 274−287.
30. Butt, J. N., Fawcett, S. E. J., Breton, J., Thomson, A., and Armstrong, F. A. (1997) *J. Am. Chem. Soc. 119*, 9729−9737.
31. Fawcett, S. E. J., Davis, D., Breton, J. L., Thomson, A. J., and Armstrong, F. A. (1998) *Biochem. J. 335*, 357−368.
32. Busch, J. L. H., Breton, J. L., Bartlett, B. M., Armstrong, F. A., James, R., and Thomson, A. J. (1997) *Biochem. J. 323*, 95−102.
33. Kyritsis, P., Huber, G. J., Quinkal, I., Gaillard, J., and Moulis, J. M. (1997) *Biochemistry 36*, 7839−7846.
34. Li, D., Agarwal, A., and Cowan, J. A. (1996) *Inorg. Chem. 35*, 1121−1125. Soriano, A., Li, D., Biar, S. M., Agarwal, A., and Cowan, J. A. (1996) *Biochemistry 35*, 12479−12486. Agarwal, A., Li, D., and Cowan, J. A. *Proc. Natl. Acad. Sci. U.S.A.* (1995), *92*, 9440−9444.
35. Bian, S., Hemann, C. F., Hille, R., and Cowan, J. A. (1996) *Biochemistry 35*, 14544−14552.
36. Butt, J. N., Armstrong, F. A., Breton, J., George, S. J., Thomson, A. J., and Hatchikian, E. C. (1991) *J. Am. Chem. Soc. 113*, 6663−6670. Butt, J. N., Sucheta, A., Armstrong, F. A., Breton, J., Thomson, A. J., and Hatchikian, E. C. (1993) *J. Am. Chem. Soc. 113*, 8948−8950. Butt, J. N., Niles, J., Armstrong, F. A., Breton, J., and Thomson, A. J. (1994) *Nat. Struct. Biol. 1*, 427−433.
37. Tong, J., and Feinberg, B. A. (1994) *J. Biol. Chem. 269*, 24920−24927.

38. Armstrong, F. A., Hill, H. A. O., and Walton, N. J. (1982) *FEBS Lett. 150*, 214−218.
39. Armstrong, F. A., Heering, H. A., and Hirst, J. (1997) *Chem. Soc. Rev. 26*, 169−179. Armstrong, F. A. (1997) in *Bioelectrochemistry of Biomacromolecules: Bioelectrochemistry: Principles and Practice* (Lenaz, G., and Milazo, G., Eds.) pp 205−235, Birkhauser Verlag, Basel. Armstrong, F. A., Butt, J. N., and Sucheta, A. (1993) *Methods Enzymol. 227*, 479−500. Armstrong, F. A. (1992) *Adv. Inorg. Chem. 38*, 117−163.
40. Duff, J. L. C., Breton, J. L. J., Butt, J. N., Armstrong, F. A., and Thomson, A. J. (1996) *J. Am. Chem. Soc. 118*, 8593−8603.
41. Moulis. J. M., and Meyer, J. (1982) *Biochemistry 21*, 4762−4771.
42. Sucheta, A., Cammack, R., Weiner, J., and Armstrong, F. A. (1993) *Biochemistry 32*, 5455−5465.
43. Hirst, J., and Armstrong F. A. (1998) *Anal. Chem. 70*, 5062−5071.
44. Heering, H. A., Weiner, J. H., and Armstrong, F. A. (1997) *J. Am. Chem. Soc. 119*, 11628−11638.
45. Xiao, Z. G., Lavery, M. J., Bond, A. M., and Wedd, A. G. (1999) *Electrochem. Commun. 1*, 309−314.
46. Hirst, J., Jameson, G. N. L., Allen, J. W., and Armstrong, F. A. (1998) *J. Am. Chem. Soc. 120*, 11994−11999.
47. Moura, I., Moura, J. J. G., Münck, E., Papaefthymiou, V., and LeGall, J. (1986) *J. Am. Chem. Soc. 108*, 349−351. Surerus, K. K., Münck, E., Moura, I., Moura, J. J. G., and Le Gall, J. (1987) *J. Am. Chem. Soc. 109*, 3805−3807.
48. (a) Srivastava, K. K. P., Surerus, K. K., Conover, R. C., Johnson, M. K., Park, J. B., Adams, M. W. W., and Münck, E. (1993) *Inorg. Chem. 34*, 927−936. (b) Finnegan, M. G., Conover, R. C., Park, J.-B., Zhou, Z. H., Adams, M. W. W., and Johnson, M. K. (1995) *Inorg. Chem. 34*, 5358−5369. (c) Staples, C. R., Dhawan, I. K., Finnegan, M. G., Dwinell, D. A., Zhou, Z. H., Huang, H., Verhagen, M. F. J. M., Adams, M. W. W., and Johnson, M. K. (1997) *Inorg. Chem. 36*, 5740−5749.
49. Frey, C. M., and Stuehr, J. (1974) in *Metal Ions in Biological Systems* (Sigel, H., Ed.) Vol. 1, p 69, Marcel Dekker, Inc., New York.
50. Armstrong, F. A., and Williams, R. J. P. (1999) *FEBS Lett. 451*, 91−94.

BI000832+